

Correlation of finite element analysis to superplastic forming experiments

S.G. Luckey Jr.^{a,*}, P.A. Friedman^a, K.J. Weinmann^b

^a Ford Motor Company, Dearborn, MI 48124, United States

^b University of California – Berkeley, Berkeley, CA, United States

Received 14 September 2006; received in revised form 21 March 2007; accepted 27 March 2007

Abstract

A simulation capability for superplastic forming has been experimentally verified. Using a long rectangular die, the predictive accuracy of two commercial finite element analysis codes has been established by correlation with superplastic forming trials from an industrial SPF process. The correlation study evaluated the FEA prediction of thickness and the bulk deformation of the sheet during forming. Based on these results, a general modeling strategy for superplastic forming has been established that provides good predictive accuracy for SPF die and process design.

© 2007 Elsevier B.V. All rights reserved.

Keywords: Superplastic forming; Finite element analysis; Aluminum sheet

1. Introduction

Superplastic forming (SPF) is a low investment process that takes advantage of certain material's ability to undergo large strains to failure when deformed under the right conditions, which usually involve elevated temperature and slow strain rates. Product development and manufacturing benefits associated with SPF include low capital investment, part consolidation and increased design freedom with materials that have limited room temperature ductility.

While modeling SPF with finite element analysis (FEA) is an essential technology for the up-front design of superplastic forming dies, the approach must be industrially practical and the level of predictive accuracy should be determined before applying FEA in die design. Although SPF modeling research with implicit and explicit finite element codes [1–4] has been published, these works do not typically provide all the necessary simulation parameters needed to accurately model SPF, nor has experimental correlation been sufficiently demonstrated. With respect to much of the published literature on SPF simulation, it is difficult to extract useful simulation parameters and methods to build and improve SPF modeling capabilities for industrial applications.

A fundamental simulation capability using commercial implicit and explicit finite element analysis codes has been estab-

lished specifically for automotive applications of SPF along with accuracy improvements in superplastic material characterization and constitutive modeling [4–11]. This work represents the experimental validation of these simulation improvements and capabilities. This research experimentally verifies an SPF simulation capability and considers many factors such as FEA solver formulation, element size, constitutive model development and the complexity of die forming surface to establish fundamental guidelines for accurately modeling industrial superplastic forming processes.

2. Material and constitutive model

The specially processed superplastic AA5083 aluminum sheet alloy used in this work was received in the fully hard condition (H19) with a nominal thickness of 1.22 mm. The constitutive model used to describe the flow stress–strain rate–strain relationship was the power law equation:

$$\sigma = K \dot{\epsilon}^m \epsilon^n \quad (1)$$

where σ is the effective flow stress, $\dot{\epsilon}$ is the effective strain rate, ϵ is the effective strain, K is a constant, m is the strain rate sensitivity exponent, and n is the strain hardening exponent. The constitutive coefficients were established using data from a high temperature tensile test. Because the high temperature tensile test does not typically employ an extensometer, an FEA based coefficient refinement technique developed by Luckey [5] has been applied that accounts for both gage section shape and the influence of material flow from the grip section on the stress, strain and strain rate. The approach is consistent with the work of Friedman and Ghosh [12], Johnson et al. [13] and Raman et al. [11]. The coefficients applied represent the superplastic response for a range of strain rates (5×10^{-4} to $3 \times 10^{-3} \text{ s}^{-1}$) that are typical of strain rates from the automotive superplastic forming of aluminum [5].

* Corresponding author. Tel.: +1 313 322 1586.

E-mail address: sluckey@ford.com (S.G. Luckey Jr.).

Nomenclature

d	initial grain size following preheat exposure prior to deformation
K	stress amplitude
m	strain rate sensitivity
n	strain hardening
o	stress exponent
p	exponent of inverse grain size

Greek letters

ε	effective strain
$\dot{\varepsilon}$	effective strain rate
σ	effective flow stress

Table 1
Coefficients for the power law constitutive model in Eq. (1)

ID	Grain size adjustment	K	m	n
a	No	187.70	0.39	0.088
b	Yes	159.50	0.39	0.088

There are aspects of the tensile test that are not fully characteristic of industrial superplastic forming processes, most notably that the tensile results represent the alloys stress-strain rate-strain response following a pre-heat (or heat-up) time of approximately 90 min within the load frame furnace. This duration of pre-heat is necessary to achieve a steady state target temperature in the tensile specimen. In automotive SPF production, the sheet may be pre-heated for no more than 5 min prior to forming to minimize cycle time. It has been documented that AA5083 experiences static grain growth when exposed to superplastic temperatures and that this grain growth influences the constitutive behavior [12,14].

This work applies a method proposed by Luckey [5] and Raman et al. [11] to relate the constitutive coefficients established from tensile test data to typical superplastic forming conditions. It assumes that the influence of initial grain size on the strain rate and strain hardening coefficients (m and n) of Eq. (1) is small and does not significantly impact FEA prediction. The dominant influence of initial grain size has been assumed to be on flow stress. This requires an adjustment to the stress term K in Eq. (1) to take into account the initial average grain size of the alloy just prior to superplastic deformation where the flow stress–initial grain size relationship can be represented by Eq. (2).

$$\left(\frac{K_1}{K_2}\right)^o = \left(\frac{d_1}{d_2}\right)^p \quad (2)$$

where K is the stress coefficient from Eq. (1), d the initial grain size associated with the duration of preheat exposure before deformation begins, p is the exponent of inverse grain size, and o is a stress exponent. The ratio presented in Eq. (2) has been derived [5,11] using the mechanistic superplasticity models of Langdon [15] and Gifkins [16].

The average initial grain size of the tensile sample, which was measured using the mean linear intercept method, with a 90 min heat-up cycle was 7.8 μm and was significantly different from sheet formed in an automotive SPF operation with a 2 min heat-up cycle where the average initial grain size was 6.6 μm [11]. Given the initial grain size following heat-up cycles of 90 and 2 min in duration and p and o are assumed to be 2 [16,17], the coefficients with and without grain size adjustment have been calculated and are provided in Table 1.

3. Experimental setup

All forming trials were done in an 800 tonnes hydraulic superplastic forming press. With a sheet loaded between the die halves and clamping force applied by the press to seal the forming cavity, gas pressure was introduced into the



Fig. 1. SPF die with long rectangle forming cavity.

lower die half forcing the sheet into the upper forming cavity. The pressure versus time curves were predicted with simulation and programmed into the press control software providing pressure control within $\pm 2\%$ of the target pressure. The thermal management system of the press uses cartridge heaters within the upper and lower platens to conduct heat into the SPF die. Automated insulated doors allow the platens and SPF die to be fully enclosed. The target forming temperature for all experiments with the SPF die was 475 $^{\circ}\text{C}$. Temperature was recorded throughout the forming cycle using the die thermocoupling and press data acquisition system. Only forming trials with an average temperature of $\pm 3^{\circ}\text{C}$ of the target temperature (475 $^{\circ}\text{C}$) were used in post-form analysis.

3.1. Superplastic forming die

The SPF die is shown in Fig. 1 and contains a long rectangular forming cavity. The cavity has a length of 600 mm, width of 200 mm, depth of 100 mm, 5 $^{\circ}$ draft angle, 10 mm entry radii and 20 mm corner (plan) radii. A radius was not applied to the bottom corner of the cavity; instead a 95 $^{\circ}$ corner exists between the bottom and vertical walls. The bottom radius of the parts formed in the cavity was set by the duration and magnitude of the gas pressure cycle.

3.2. Blank size and lubrication

All blanks were sheared from the same lot of material. The blank size was 810 mm by 460 mm with the rolling direction perpendicular to the long axis of the blank. Each blank was coated on both sides with a proprietary Ford Motor Company SPF lubricant that contains boron nitride. This solid lubricant is capable of withstanding the temperature range (450–550 $^{\circ}\text{C}$) employed in aluminum superplastic forming. It is effective at preventing the sheet from sticking to the die and thus assists in the forming of the sheet and acts as a parting agent during part extraction.

3.3. Forming process

Each blank was preheated external to the press within a proprietary automated preheat and blank loading apparatus. The preheat was necessary to both recrystallize the fully hard material and heat the blank to the target temperature for gas forming. The preheat system also automatically loaded each blank into the press. The duration of blank preheat was 2 min which is consistent with Friedman et al. [18] where the sheet was found to fully recrystallize and achieve the target forming temperature within 60 s.

4. Finite element analysis

The simulation approach and parameters applied in this work are consistent with those evaluated previously in the works cited [5–9]. The die was modeled with the commercial FEA codes ABAQUS/Standard (implicit) and LS-DYNA (explicit), where 3-D finite element analysis was applied in the correlation of simulation to experimental forming trials. Independent of the

FEA code, a number of common simulation parameters were applied in modeling the SPF of the die cavity.

In ABAQUS and LS-DYNA, a viscoplastic formulation of the constitutive model was applied using the power law equation (Eq. (1)). The coefficients applied in this work are shown in Table 1. The significance of each set of coefficients is discussed in Section 2.

Convergence difficulties can be experienced when modeling superplastic forming with ABAQUS due to highly non-linear contact conditions. To address convergence problems it was necessary to apply “softened” contact to the pressure–overclosure relationship of ABAQUS. Within LS-DYNA, surface to surface contact was used to define the contact interface between the sheet and die.

The Coulomb friction model in Eq. (3) was used to define the frictional behavior in both FEA codes.

$$\tau = \mu P \quad (3)$$

where the coefficient of friction (μ) and normal contact pressure (P) define the critical shear stress (τ) at which sliding between contacting surfaces can begin. Efforts to define the frictional behavior of the solid lubricants commonly applied in SPF have been conducted [19,20]; however, definitive correlation to simulation has not been established. Friedman et al. [21] developed a high temperature sliding friction test apparatus that can be effectively used to screen solid lubricants used in SPF. In evaluating the SPF lubricant described in Section 3.2, a coefficient of friction was calculated for each of six friction tests [21]. The average μ was calculated to be 0.16 and was used in all FEA models.

4.1. Explicit FEA simulation parameters

It was demonstrated by Luckey et al. [9] that with the appropriate explicit FEA simulation parameters an explicit FEA code such as LS-DYNA can model SPF and provide an equivalent solution to the quasi-static results of ABAQUS Standard. The explicit simulation parameter applied in LS-DYNA was a mass scale factor of 10^5 .

4.2. Mesh and boundary conditions

The forming surface of the die was meshed using the tool meshing capability of DYNAFORM version 5.1. The blank was defined with a uniform mesh size using shell elements with reduced integration. The nodes on the perimeter of each blank were constrained to simulate the clamping of the sheet between the die halves during gas forming.

The influence of element size was evaluated in this study based on the results of Venkateswaran et al. [10]. It has been previously established [7] that conventional shell elements are not as effective as layered solid element in predicting the through thickness behavior of superplastic materials. Although shells have difficulty predicting an important failure mode of superplastic forming, where sheet is gas formed over a small radius, they are more computationally viable for 3D analysis. Given

Table 2
Optimum ratio of element size to radius as a function of entry radius [10]

Radius (mm)	Element size/radius
5	3/5
10	3/5
15	2/5

the limitations of shells, Venkateswaran used numerical experiments to establish an element size guideline for modeling SPF that offers the best shell element thickness prediction performance providing the minimum computation time. Because the smallest radius formed over within a die cavity is the critical aspect influencing the thickness profile prediction, a minimum ratio of element size to forming radius was established for various forming (entry) radii for a plane strain rectangular forming cavity. These ratios are provided in Table 2. Based on these results, Venkateswaran et al. established a general ratio of 2/5 for use in 3-D SPF simulation. The applicability of these finding to explicit FEA and correlation to experiment will be discussed in Sections 6 and 7.

4.3. Gas pressure cycle

The gas pressure cycle was predicted using a subroutine specially developed for superplastic forming. The function and execution of the algorithm is consistent with other work in the literature [10,22,23]. The algorithm employs an averaging scheme to predict the gas pressure history needed to maintain a target strain rate within the deforming sheet. During forming simulation, the strain rates of the elements with the highest 5% of strain rates are ignored and the elements with the next highest 20% of strain rates are averaged. This average is used to adjust pressure dynamically during simulation to maintain a predefined target strain rate through out the forming cycle.

4.4. Correlation guidelines

For this work, good correlation in thickness prediction between simulation and experiment was achieved for a maximum difference of no greater than 5% between predicted and experimentally measured thinning. The correlation in bulk sheet deformation into the cavity has been considered good when the difference between the predicted and experimental sheet bulge height is less than 5 mm.

5. Experimental results

Three panels were completely formed at a target strain rate of 10^{-3} s^{-1} . Thickness was measured at the locations identified in Fig. 2 and the percent thinning calculated. Location T1 corresponds to the mid-point of the bottom face, locations T2 and T3 are on the mid-point of the front and back sides and T4 and T5 are on the mid-point of the left and right sides. The initial thickness of each panel was measured prior to forming and used in the calculation of percent thinning. All thickness measurements were done with an ultrasonic thickness gage with a 3.5 mm diameter probe. The measured thickness and percent thinning results were averaged and are shown in Table 3. Due to the symmetry of the part, the adjacent locations T2, T3 and T4, T5 were averaged, respectively. The coefficient of variation (COV) was calculated for each set of thickness measurement and

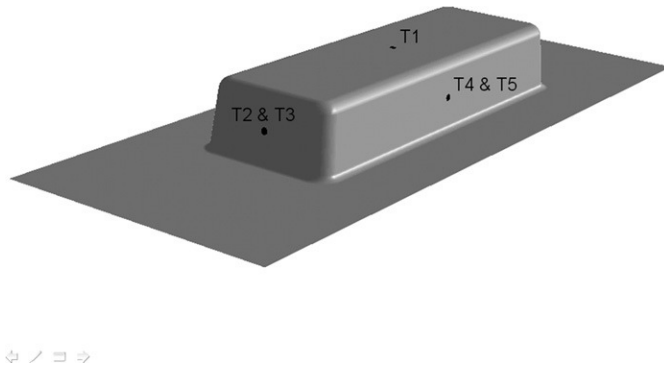


Fig. 2. Location of thickness measurements on formed panels.

has been shown in Table 3. The scatter in the thickness data was reasonably low with a maximum COV of 2.2%.

A series of interrupted tests were performed where the gas forming cycle was stopped at 25, 50, 150, 250, 350, 550 and 885 s. At 885 s, the part was considered fully formed with a bottom radius of 20 mm along the long axis. Three replicates were formed for each time and the maximum depth of the bulge into the cavity measured with a height gage. The data were averaged and the COVs calculated (see Table 4). For the forming times 550 and 885 s, all panels had reached the bottom of the 100 mm deep die cavity. The calculated COVs indicate low scatter among the measured forming depth data except for the 50 s tests. For that data set, one panel was 4 mm deeper than the other two panels. This panel was formed with an average die temperature of 478 °C, while the other two panels were formed at 475 °C. Given the strong influence of temperature on superplastic deformation, especially with respect to flow stress, it is not surprising the panel went further into the cavity. The panel was included in the calculation of the average forming depth because it was formed within the temperature tolerance of ± 3 °C.

The results of the forming trials were compared to the predicted results of LS-DYNA and ABAQUS with respect to thickness and deformation. The FEA conditions applied in the correlation study are listed in Table 5. Conditions 1 and 2 corresponded to LS-DYNA and ABAQUS models where the fixed mesh size guideline discussed in Section 4.4 prescribed an element size of 4 mm. The impact of neglecting the effects of thermal expansion on SPF simulation was also considered in condition 3. The thermal expansion factor applied to the die geometry was 1.012 and corresponded to heating the 4140 steel SPF dies to

Table 3
Average experimental thickness and percent thinning at the formed panel locations identified in Fig. 2

	Average thickness (mm)	COV (%)	Average thinning (%)
T1	0.76	2.2	38.2
T2 and T3	0.74	1.6	39.6
T4 and T5	0.76	1.0	38.7

Table 4
Average forming depth of blanks into the long rectangular cavity and the corresponding forming time

Forming time (s)	Average forming depth (mm)	COV (%)
25	28	2.0
50	37	7.2
150	60	1.0
250	78	2.7
350	93	0.6
550	100	0.0
885	100	0.0

Table 5
FEA conditions for experimental correlation

ID	Condition
1	LS-DYNA, rate: 10^{-3} s^{-1} , element size: 4 mm, constitutive coefficients: <i>b</i>
2	ABAQUS, rate: 10^{-3} s^{-1} , element size: 4 mm, constitutive coefficients: <i>b</i>
3	LS-DYNA, rate: 10^{-3} s^{-1} , element size: 4 mm, constitutive coefficients: <i>b</i> , CTE applied
4	LS-DYNA, rate: 10^{-3} s^{-1} , element size: 4 mm, constitutive coefficients: <i>a</i>
5	LS-DYNA, rate: 10^{-3} s^{-1} , element size: 2 mm, constitutive coefficients: <i>b</i>
6	LS-DYNA, rate: 10^{-3} s^{-1} , element size: 6 mm, constitutive coefficients: <i>b</i>
7	LS-DYNA, rate: 10^{-3} s^{-1} , element size: 10 mm, constitutive coefficients: <i>b</i>
8	LS-DYNA, rate: 10^{-2} s^{-1} , element size: 4 mm, constitutive coefficients: <i>b</i>

475 °C. Condition 3 was compared to experiment as well as models 1 and 2 to establish if it is necessary to include the thermal expansion of the die during SPF in simulation.

Unless otherwise noted the constitutive coefficients labeled (b) in Table 1, which consider the effect of average initial grain size, were applied in FEA. The unadjusted coefficients labeled (a) in Table 1 were applied in condition 4. The accuracy improvements attained by considering the average initial grain size in constitutive model development has been assessed by comparing conditions 1 and 4.

Conditions 6, 7 and 8 used element sizes 2, 6 and 10 mm, respectively (corresponding to element size/radius ratios 1/5, 3/5 and 1) to define the blank mesh. Hence, the element size guidelines of Vekateswaran et al. [10] were evaluated by comparing these results and the results from condition 1 to the experimental data. Finally, in condition 8 an LS-DYNA model was run with a target strain rate of 10^{-2} s^{-1} . The thickness locations identified in Fig. 2 were recorded and compared to those predicted with condition 1. Condition 8 was used to evaluate the effects of velocity scaling on thickness prediction. This result is relevant to the development of an overall simulation strategy for computationally efficient FEA driven SPF die design that is discussed in Section 7.7.

Thickness was also measured across sections of one panel perpendicular (Fig. 3(a)) and parallel (Fig. 3(b)) to the long axis of the part. Measurement began at the center of the bottom of the pan. Subsequent measurements were made every 10 mm except at the bottom and top radii where the spacing was

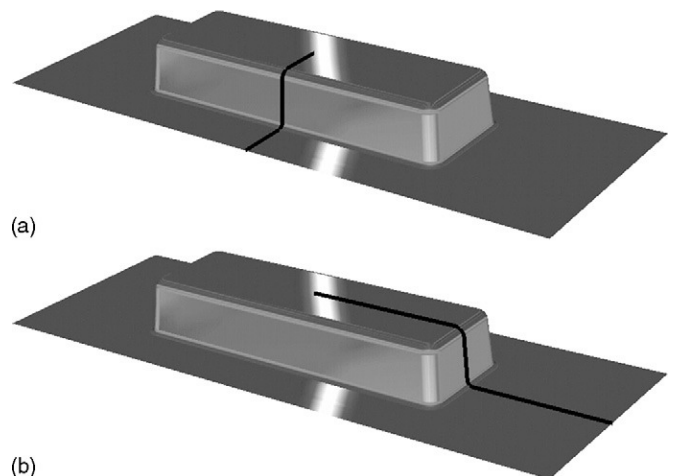


Fig. 3. Thickness profiles measured experimentally and in FEA along sections perpendicular (a) and parallel (b) to the length of the part.

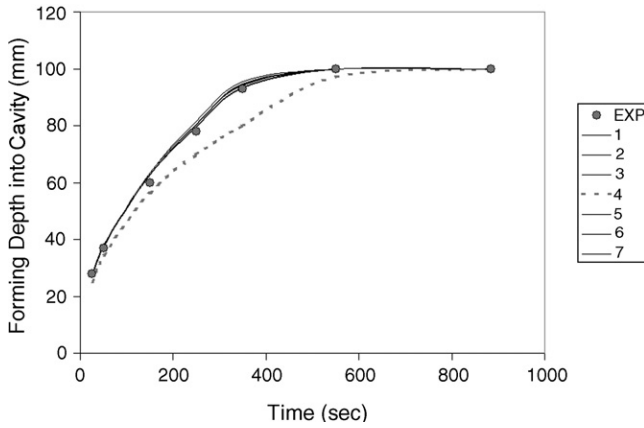


Fig. 4. Forming depth of sheet into the die cavity with respect to time.

5 mm. These thickness profiles were compared to the thickness profiles predicted with element to entry radius ratios 1/5, 2/5, 3/5 and 1. This analysis represents an additional evaluation of the element size guidance of Venkateswaran et al. [10].

For the FEA conditions described above, the same pressure cycle was applied in conditions 1 through 7. However, another aspect of superplastic forming simulation is the influence of element size on the prediction of the forming cycle. Applying the entry radius ratios 1/5, 2/5, 3/5 and 1, gas pressure cycles for forming at a target strain rate of $2 \times 10^{-3} \text{ s}^{-1}$ were predicted and compared. The results were used to establish general guidelines of element size selection for process design (i.e. the development of the SPF gas pressure cycle).

6. Correlation results

The predicted thinning at the locations identified in Fig. 2 for the conditions outlined in Table 5 are compared to the average experimental percent thinning in Table 6. In general, FEA predicted slightly more thinning than was experimentally measured. The maximum deviation from experiment was 2.4% for condition 4 at locations T4 and T5 which is within the guideline stated in Section 4.4 of 5% used to define good correlation.

In Fig. 4, the measured depth of the sheet into the cavity as a function of forming time was compared to the sheet depth predicted with FEA for the conditions in Table 5. All FEA conditions fall within the guideline for good correlation (from Section 4.4) except condition 4. Not considering condition 4, the greatest difference between predicted and experimentally observed forming depth was 3.6 mm for conditions 3 and 7 at 150 s.

The experimentally measured thickness profiles identified in Fig. 3(a) and (b) and the predicted profiles for the different element sizes defined by the element size to entry radius ratios 1/5, 2/5, 3/5 and 1 are shown in Figs. 5 and 6. For all except ratio 1, the FEA results differ from experiment by less than 5% and are

Table 6
Experiment and predicted percent thinning at the locations identified in Fig. 2

Location ID	Condition								
	Exp. (%)	1 (%)	2 (%)	3 (%)	4 (%)	5 (%)	6 (%)	7 (%)	8 (%)
T1	38.2	38.5	37.5	37.8	39.2	38.4	38.5	38.4	37.6
T2 and T3	39.6	41.0	40.6	40.2	41.2	41.6	41.2	40.1	39.8
T4 and T5	38.7	40.7	39.7	40.2	41.1	40.9	40.8	40.0	39.7

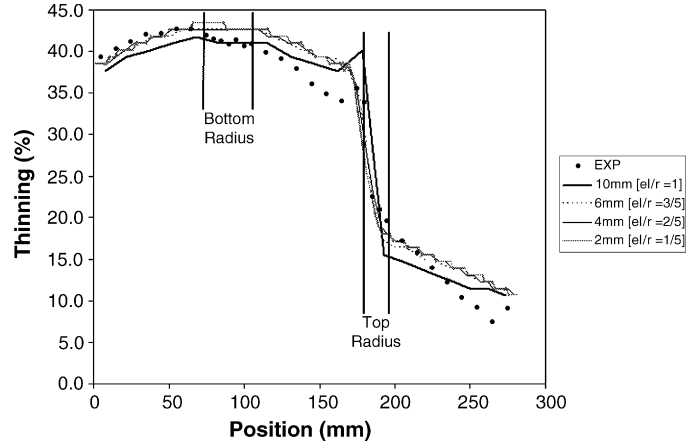


Fig. 5. Experimentally measured and FEA predicted thickness profiles perpendicular to the length of the die cavity. Position from left to right represents length of line distance from the center of the cavity to the die flange.

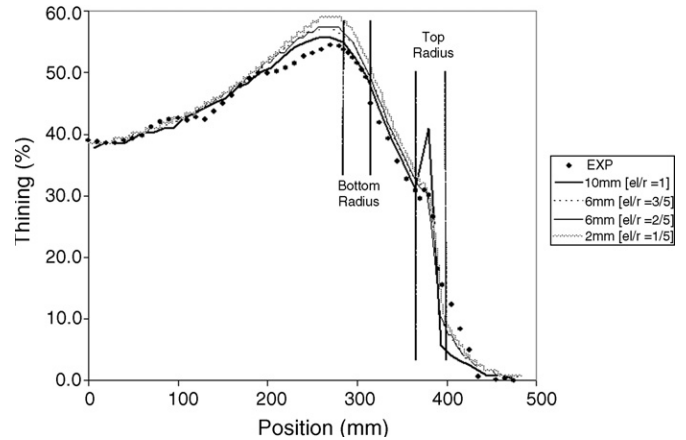


Fig. 6. Experimentally measured and FEA predicted thickness profiles parallel to the length of the die cavity. Position from left to right represents length of line distance from the center of the cavity to the die flange.

considered to have good correlation. In Table 7, a correlation coefficient (U^2) was calculated to further compare the predicted profile of each element size to the measured profile shown in Fig. 5. This correlation coefficient is the square of the Pearson product moment correlation coefficient and has been used in this work to measure the proportion of the variance between the FEA and experimental data sets. Table 8 provides the U^2 terms for the results in Fig. 6.

The influence of element size on the prediction of the forming cycle has also been evaluated. Pressure curves were predicted for a target strain rate of $2 \times 10^{-3} \text{ s}^{-1}$ using different mesh sizes of 2, 4, 6 and 10 mm corresponding to the element size/entry radius

Table 7
 U^2 terms for data in Fig. 5 comparing the correlation of thickness profiles predicted respective of element size to experiment

Element size (mm)	Element size/radius	U^2
2	1/5	0.97
4	2/5	0.97
6	3/5	0.97
10	1	0.95

Table 8
 U^2 terms for data in Fig. 6 comparing the correlation of thickness profiles predicted respective of element size to experiment

Element size (mm)	Element size/radius	U^2
2	1/5	0.99
4	2/5	0.99
6	3/5	0.99
10	1	0.97

ratios 1/5, 2/5, 3/5 and 1. Each simulation concluded when 99% of the blank nodes were in contact the die surface. The predicted pressure cycles are plotted in Fig. 7.

7. Discussion

7.1. Correlation of implicit and explicit FEA

By comparing conditions 1 and 2 in Table 6 and Fig. 4 to experimental results, it can be seen that LS-DYNA and ABAQUS not only demonstrate good correlation to each other but also to experiment. In general, LS-DYNA achieved a faster computation time and reached a converged solution more often. Based on this as well as the predictive agreement between the implicit and explicit FEA codes in Luckey [5], an explicit FEA code such as LS-DYNA can provide a reliable and more robust solution and is well suited to industrial simulation driven die design for superplastic forming.

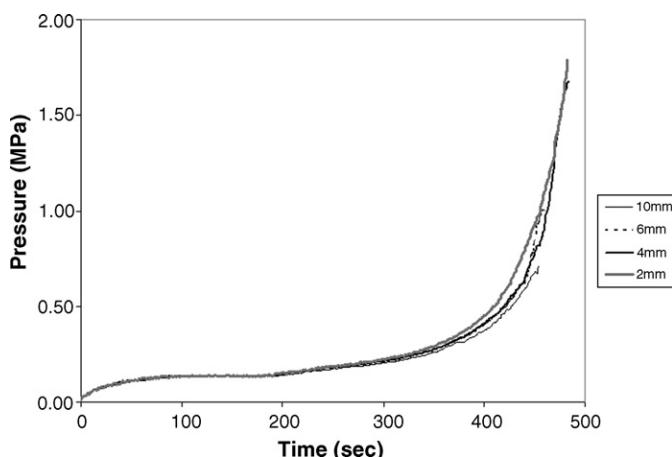


Fig. 7. Predicted pressure vs. time cycles for forming a sheet at a strain rate of $2 \times 10^{-3} \text{ s}^{-1}$ respective of element size.

7.2. Thermal expansion

Conditions 1 and 3 in Table 6 and Fig. 4 demonstrate that the effects of thermal expansion on the die and blank geometry did not provide a significant improvement or change in FEA prediction. Therefore, it is not necessary to consider thermal expansion in SPF simulation for the forming conditions and materials used in this work.

7.3. Constitutive model development

The performance of the constitutive coefficients in Table 1 are compared to experiment in Table 6 and Fig. 4 by considering conditions 1 and 4. Although both conditions provide good thickness prediction that did not differ from experimental results by more than 2%, condition 4 provided poor prediction of sheet deformation into cavity. It is concluded that initial grain size should be considered in developing the constitutive coefficients. That thickness was well predicted by both models validates the approach of Luckey [5] and Raman et al. [11] outlined in Section 2, where a flow stress–grain size relationship was derived that adjusts flow stress via the K coefficient and neglected the effect of grain size on strain rate sensitivity and strain hardening. Based on these results, the power law constitutive model may be applied in SPF simulation and the FEA based coefficient refinement and grain size adjustment methods were effective in establishing the constitutive coefficients.

7.4. Influence of element size on thickness prediction

In Table 6, conditions 1,5,6 and 7 do not demonstrate significant influence of element size on thickness prediction at the locations identified in Fig. 2. However, Venkateswaran et al. [10] reported that the greatest influence of element size in predicting thickness in SPF occurs in regions of the die cavity where sheet is forming over radii. Predicted and experimentally measured thickness profiles for sections at the middle of a panel parallel and perpendicular to the long axis of the long rectangular die in Figs. 5 and 6 verify this finding. It is clear that as element size increases (especially to a ratio of 1) predictive capability near the entry radius degrades. In fact, for both sections in Figs. 5 and 6 the entry radius for ratio 1 was the only location to exceed the correlation guideline on thinning defined in Section 4.4.

Based on the numerical experiments of Venkateswaran et al. [10], a general element size to entry radius ratio of 2/5 was recommended; however, when specifically considering a 10 mm entry radius Venkateswaran found a 3/5 ratio acceptable (see Table 2). Given that the entry radius of the long rectangular die cavity was 10 mm a direct comparison can be made by means of a correlation coefficient. In Tables 7 and 8, a correlation coefficient (U^2) was used to compare FEA prediction and experiment for each ratio of element size and entry radius. This measure was used to identify the ratio for which the solution begins to degrade as compared to experiment. For the thickness profiles the minimum U^2 terms are 0.95 and 0.97 for a ratio of 1. Ratios 1/5, 2/5 and 3/5 had the same correlation coefficient of 0.99, suggesting that for this geometry a maximum ratio of 3/5 may

be applied in simulation without significant loss of predictive accuracy. This result provides correlation of FEA to experiment that supports the conclusions of Venkateswaran et al. [10].

7.5. Numerical influence of element size on sheet deformation

The influence of element size on the predicted bulk deformation of the sheet into the cavity given a predefined pressure curve is shown in Fig. 4. No significant difference was observed as a function of element size. Using the LS-DYNA strain rate control algorithm, a gas pressure cycle was predicted for each element size and the resulting curves are shown in Fig. 7. The curves are nearly identical up until the end of the gas cycle, where it was observed that models with more elements had longer predicted gas cycles and higher final pressures. This can be attributed to the function of the strain rate control algorithm. The algorithm ends the simulation when 99% of the sheet nodes are in contact with the die cavity. The finer meshed sheet required a longer forming time and higher pressures to drive it further into the bottom corners of the cavity to achieve the nodal contact criterion.

7.6. Numerical influence of strain rate on thickness prediction

For the long rectangular die cavity, a pressure curve was predicted for condition 8 for a target strain rate of 10^{-2} s^{-1} . The thicknesses predicted for the locations identified in Fig. 2 are shown in Table 6. Since there was no significant difference between the thicknesses predicted with condition 8 and condition 1, strain rate does not appear to significantly influence FEA thickness prediction. Although contrary to experimental observations of superplasticity, this was the result of the constitutive assumptions applied in finite element analysis. In this formulation there is no mechanism in the simulation to model the reduced rate sensitivity of the material at higher strain rates. Instead, both FEA conditions used the basic constitutive equation in Eq. (1) and the same set of constitutive coefficients; hence, nearly the same thickness distribution was predicted. This behavior was also observed by Harrison et al. [6] using ABAQUS.

In effect, by increasing the target strain rate from 10^{-3} s^{-1} to 10^{-2} s^{-1} , a limited level of velocity scaling was applied. Velocity scaling is a common method applied in stamping simulation with explicit FEA where the punch velocity is artificially increased to reduce the computation time of the simulation. It is an alternative and essentially equivalent to the mass scaling applied in Luckey et al. [9], and like mass scaling, too much velocity scaling introduces error into the solution. To predict an accurate pressure curve with LS-DYNA, the mass scale factor applied in Luckey et al. [9] should be applied without velocity scaling. However, based on the results with the rectangular die cavity an accurate thickness profile can be predicted with a target strain rate of 10^{-2} s^{-1} . This offers some advantages because an explicit FEA model with a target strain rate of 10^{-2} s^{-1} is less computationally intensive than an explicit FEA model with a target strain rate of 10^{-3} s^{-1} .

7.7. Simulation driven die design for superplastic forming

Based on the results of this work, it is proposed that SPF simulation be separated into two steps: die design and process development. During SPF feasibility and die design, 3-D analysis with LS-DYNA is done with a limited level of velocity scaling, where the target strain rate is at most 10^{-2} s^{-1} and employing the mesh guideline ratio of 2/5. With this approach computation time is reduced enabling iterative SPF die design for achieving an optimum thickness profile.

Significant computation time is required to predict the gas pressure cycle for a strain rate of 10^{-3} s^{-1} using the mesh guideline ratio of 2/5. If a die has been designed to provide an acceptable thickness profile, a second step of process development may be employed to predict the SPF gas forming cycle process with reasonable computational efficiency. In Section 6, a blank mesh of 10 mm (element size to radius ratio of 1) predicted nearly the same pressure curve as a 2 mm mesh; however, in practice, additional pressure and time would likely be needed at the end of the 10 mm pressure curve to complete the forming of the component. Based on this result, the process design for SPF may be done using a coarser mesh with an element size ratio of 1 as compared to a ratio of 2/5 for die design.

8. Conclusions

Superplastic forming simulation using finite element analysis was correlated to experimental forming trials. The results and conclusions of this work represent the verification of a fundamental simulation capability suitable for up-front SPF die design. Conclusions are as follows:

- Both the implicit code ABAQUS and explicit code LS-DYNA may be used to accurately model the thinning and bulk deformation of aluminum sheet during superplastic forming.
- The power law equation can be used as a constitutive model for superplastic forming. The constitutive model coefficients established with the iterative refinement and grain size adjustment methods developed by Raman et al. [11] and Luckey [5] provide good characterization of superplastic sheet forming.
- The mesh size guidelines of Venkateswaran et al. [10] demonstrate good correlation to experiment and can be applied in explicit FEA.
- To apply simulation to SPF die design the development process may be broken into two steps of die design and process development. In addition to a mass scale factor of 10^5 , a limited amount of velocity scaling can be applied in die design with a mesh guideline ratio of 2/5. In process development, the pressure curve can be predicted using a coarser mesh with an element size to radius ratio of at most 1.

Acknowledgements

The authors would like to thank Ford Motor Company for funding this research and Richard Allor, Warren Copple and Craig Miller for their efforts in both experimental forming trials and material characterization.

References

- [1] R.D. Wood, J. Bonet, A Review of the Numerical Analysis of Superplastic Forming, *J. Mater. Process. Technol.* 60 (1996) 45–53.
- [2] C. Kim, M.G. Konopnicki, F.G. Lee, SSR fender produced by math-based technology, in: E.M. Taleff, al. et (Eds.), *Advances in Superplasticity and Superplastic Forming*, TMS, 2004, pp. 77–82.
- [3] G.K. Young, L. Firth, G. Glenn, F. Gillespie, Superplastic Forming Analysis for Tool Design and Process Development, in: *Proceedings of First SAE Aerospace Manufacturing Technology Conference*, SAE Report no. 972223, Seattle, WA, 1997.
- [4] F. Lee, K. Murali, A. Heath, R. Gandikota, Simulation based development of quick plastic forming, SAE Paper no. 2005-01-0088, Society of Engineers Int. Congress and Exposition, Detroit, MI, 2005.
- [5] S.G. Luckey, Development of finite element analysis based tools and methods for the design of advanced superplastic forming dies and processes, Ph.D. thesis, Michigan Technological University, Houghton, MI, 2006.
- [6] N.R. Harrison, S.G. Luckey, P.A. Friedman, Z.C. Xia, Influence of friction and die geometry on simulation of superplastic forming of Al–Mg alloys, in: E.M. Taleff, al. et (Eds.), *Advances in Superplasticity and Superplastic Forming*, TMS, 2004, pp. 301–309.
- [7] S.G. Luckey, P.A. Friedman, Z.C. Xia, Aspects of element formulation and strain rate control in the numerical modeling of superplastic forming, in: E.M. Taleff, al. et (Eds.), *Advances in Superplasticity and Superplastic Forming*, TMS, 1994, pp. 371–380.
- [8] S.G. Luckey, P.A. Friedman, C. Xia, K.J. Weinmann, Correlation of implicit finite element analysis to superplastic forming experiments, *Trans. NAMRI/SME* 33 (2005) 33–40.
- [9] S.G. Luckey, P.A. Friedman, C. Xia, K.J. Weinmann, Simulation of superplastic forming using explicit finite element analysis, *Trans. NAMRI/SME* 34 (2006) 33–37.
- [10] V. Venkateswaran, S.G. Luckey, G. Kridli, P.A. Friedman, Accuracy and efficiency issues related to element size and pressure control in superplastic forming, *Trans. NAMRI/SME* 34 (2006) 25–32.
- [11] H. Raman, S.G. Luckey, P.A. Friedman, G. Kridli, Development of accurate constitutive models for simulation of superplastic forming, *J. Mater. Eng. Perform.* 16 (2007) 284–292.
- [12] P.A. Friedman, A.K. Ghosh, Control of superplastic deformation rate during uniaxial tensile tests, *Metall. Mater. Trans. A* 27A (1996) 3030–3042.
- [13] K.I. Johnson, M.A. Khaleel, C.A. Lavender, M.T. Smith, Accuracy issues in modeling superplastic metal forming, in: A.K. Ghosh, T.R. Bieler (Eds.), *Superplasticity and Superplastic Forming*, TMS, 1995, p. 197.
- [14] H. Iwasaki, K. Higashi, S. Tanimura, T. Komatubara, S. Hayami, Superplastic deformation characteristics of 5083 aluminum alloy, in: *Superplasticity in Advanced Materials*, The Japan Society for Research on Superplasticity, 1991, pp. 447–452.
- [15] T.G. Langdon, A Unified approach to grain boundary sliding in creep and superplasticity, *Acta Metall.* 42 (1994) 2437–2443.
- [16] R.C. Gifkins, Grain-boundary sliding and its accommodation during creep and superplasticity, *Metall. Trans. A* 7A (1976) 1225–1232.
- [17] T.G. Langdon, The Physics of superplastic deformation, *Mater. Sci. Eng.* A137 (1991) 1–11.
- [18] P.A. Friedman, C. Miller, R.L. Allor, W.B. Copple, Development of contact pre-heater for superplastic forming of aluminum sheet, Ford Internal Technical Report, 2005.
- [19] R.W. Davies, M.A. Khaleel, S.G. Pitman, M.T. Smith, Experimental determination of the coefficient of friction during superplastic forming of AA5083 aluminum alloy, in: D.C. Duhnanad, D.G. Sanders (Eds.), *Proceedings of First and Second International Symposia on Superplasticity and Superplastic Forming*, ASM International, 2001/2002, pp. 39–43.
- [20] R.B. Kelly, S.B. Leen, I.R. Pashby, A.R. Kennedy, in: R.I. Todd (Ed.), *The Measurement of Friction for Superplastic Forming of Ti-6Al-4V*, Superplasticity in Advanced Materials, Trans Tech. Pub., 2003, pp. 111–116.
- [21] P.A. Friedman, W.B. Copple, R.L. Allor, S.G. Luckey, High temperature lubricant test for superplastic forming, *Trans. NAMRI/SME* 33 (2005) 25–31.
- [22] K. Murali, P. Montgomery Jr., J.G. Schroth, Development of Marc for analysis of quick plastic forming processes, in: E.M. Taleff, al. et (Eds.), *Advances in Superplasticity and Superplastic Forming*, TMS, 2004, pp. 311–321.
- [23] M.A. Khaleel, K.I. Johnson, C.H. Hamilton, M.T. Smith, Deformation modeling of superplastic AA-5083, *Int. J. Plast.* 14 (1998) 1133–1154.